Replica Symmetry Breaking in Colloidal Plasmonic Random Laser with Gold Coated Triangular Silver Nanostructures

ARINDAM DEY,[1] ASHIM PRAMANIK,[1] KOUSHIK MONDAL,[1] SUBRATA BISWAS,[1] UDIT CHATTERJEE,[3] FABRIZIO MESSINA,[2] PATHIK KUMBHAKAR[1,*]

[1]*Nanoscience laboratory, Dept. of Physics, National Institute of Technology Durgapur, 713209, West Bengal, India.*
[2]*Dipartimento di Fisica e Chimica – Emilio Segrè, Università degli Studi di Palermo, Via Archirafi 36, Palermo, 90123 Italy.*
[3]*Laser Laboratory, Dept. of Physics, The University of Burdwan, Burdwan, 713104, India.*
**Corresponding author: pathik.kumbhakar@phy.nitdgp.ac.in*

Received XX Month XXXX; revised XX Month, XXXX; accepted XX Month XXXX; posted XX Month XXXX (Doc. ID XXXXX); published XX Month XXXX

Plasmonic random lasers are becoming attractive alternatives, due to their versatility, low threshold, and possibility of having tunable and coherent/incoherent outputs. However, in this Letter, the phenomenon of replica-symmetry-breaking is reported in intensity fluctuations of a rarely used colloidal plasmonic random laser (RL) system. Triangular nanosilver particles provide incoherent RL action when used in the DMF environment for gain medium of Rhodamine-6G. The substitution of gold coated triangular nanosilver with triangular nanosilver within the RL system offers dual contribution of scattering and lower photo reabsorption, which leads to a drastic reduction of the lasing threshold energy by 39% as compared to that with the later. Further, due to its long-term photostability and chemical properties, photonic paramagnetic phase to glassy phase transition is observed in the used colloidal plasmonic RL system. Remarkably, the transition occurs approximately at the lasing threshold value which is a consequence of stronger correlation of modal behaviors at high input pump energies.

Random lasers (RLs) are a new class of laser sources in which the active medium consists of fluorophore mixed with a disordered material, providing random propagation of light through scattering [1]. RLs do not possess any 'precisely aligned mirror' cavity system; instead, light is scattered multiple times randomly within the gain medium before it is amplified and emitted, resulting in spatially and temporally chaotic output. That is why they are also termed as 'chaotic laser' or 'disordered laser'. Here, the arbitrarily distributed micro/nano structures over space provide the prerequisite feedback of light, via a range of internal processes ultimately due to light scattering: photon diffusion [2], localization [3], multiple scattering [4], extended amplified modes [5], external feedbacks [6,7] etc. Many disordered systems have been employed to show random lasing, since Letokhov's [8] original prediction in 1968. Since then, different exotic nanostructured systems based on dye-doped metal nanostructures [9], carbon dots [10], photonic crystals [11], metal organic frameworks [12], perovskites [13,14], silk based biocompatible substances [15, 16], and other bio-extracted substances [17-19] have been shown to exhibit RL emission. In particular, noble metal nanoparticles have gained considerable attention in the RL community due to some unique properties like their easily synthesizable different structures, versatile optical responses over the whole electromagnetic spectrum along with remarkable surface plasmon resonance (SPR) properties. Among the noble metal nanostructures, silver (Ag) and Gold (Au) are the most prevalent for their employment in RL experiments [20-22]. However, in a recent study authors have utilized SPR properties of TiN nanoparticles to achieve coherent RL emission in a laser dye [23].

One of the most characteristic features of RLs is that they display large shot-to-shot intensity fluctuations due to the inherent random scattering of light by scatterers within the RL media. These fluctuations are often described by statistical measures such as the degree of intensity correlation and the probability density function of the laser output. Due to the non-deterministic nature of RLs, their performance can be indeed difficult to predict, and their output may vary significantly from device to device or over time. However, the statistical behavior of RL can be described with statistical mechanical methods borrowed by spin glass theory (SGT) [24]. The SGT is one of the prime and fascinating paradigms of statistical mechanics for complex physical systems and found applications in a wide range of various disciplines of study. One very interesting aspect of SGT is the phenomenon of replica symmetry breaking (RSB), initially developed by Edwards and Anderson. RSB is a notion that discusses how identical systems prepared under identical circumstances can achieve distinct equilibrium states. Thus, RSB provides a way to analyze the statistical properties of the system and identify the presence of multiple solutions or minima in the energy landscape which are related to its phase transitions. Hence, it plays a key role in determining the thermodynamic and dynamic properties of the system. In a RL

experiment, the lasing modes are considered in analogy to continuous complex spin variables having some constraints, and their coupling is determined by the interaction of disorder and nonlinearity in accordance with the SGT. On the contrary, the injected pump energy into the RL system plays the role of inverse temperature as in case of thermodynamical equilibrium, and the transition from fluorescence emission to RL can be seen as a phase transition analogous to that from photonic paramagnetic system to the spin glass phase. Recently, the RSB phenomenon in RL has been first experimentally verified by Ghofraniha *et al.* [25]. After this initial report, a few more studies on RSB in various RL configurations have been published, such as in optofluidic RL system [26], powder laser systems [27,28] etc. However, RSB in liquid phase RL system remains very rare and difficult to achieve. Recently, Pincheira *et al.* reported RSB in ethanolic solution of specially functionalized TiO_2 nanoparticles [31]. In their experiment, a long-term stability (~10^4 laser shots) of the nanoparticle suspension is shown, such that the disordered system can be considered to be frozen throughout the time of observation, which is mandatory to apply the conceptual framework of RSB. Further, $ZrTe_2$ based suspension [32] has been shown to exhibit RSB phenomenon in a liquid phase. So, there has been a trend of searching for possible RSB in liquid phases where the system can be taken to be identical throughout the duration of observation. Although only a few reports of RSB in liquid phases have recently been appeared [29-32], however RSB in plasmonic nanoparticle-based liquid RL system has not been reported yet.

Therefore, in this work, we report about RL action in DMF solution of Rhodamine-6G (R6G) dye, achieved by using triangular silver nanoparticles (TSN) and Au coated TSN as nano-scatterers for amplification of light. We find RL action with three different colloidal scatterer solutions consisting of bare TSN (TSN1), 3 nm Au shell coated TSN (TSN2) and 6 nm Au coated TSN (TSN3). While efficient RL action is induced on R6G by all three scatterers, 39% reduction in lasing threshold energy (E_{in}^{th}) is achieved when TSN1 scatterer is substituted by TSN3 scatterer. Notably, we provided here, for the first time, clear evidence of RSB phenomenon in a colloidal plasmonic RL configuration. The results are relevant for ongoing investigations on colloidal RLs, and may pave the way for further research on disordered structures.

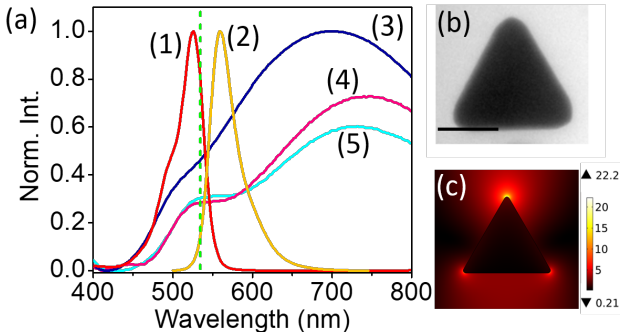

Fig. 1. (a) (1) UV-Vis. abs. spectra of DMF solution of R6G dye and (2) PL emission spectra of R6G dye in DMF environment under 532 nm excitation (shown in green dashes). Absorption spectra of (3) TSN1 sample, (4) TSN2 sample, (5) TSN3 sample. (b) TEM image of TSN1 (scale bar is 50 nm) sample and (c) corresponding simulated electric field distribution image under 532 nm excitation.

The syntheses procedures of the TSN1, TSN2 and TSN3 have been reported earlier by our research group [33]. The optical properties of the gain and scatterer media are depicted in Fig. 1 (a). As an amplifying media, 0.5 mM concentration of R6G dye in DMF solvent has been taken. The UV-Visible absorption (UV-Vis. abs.) spectra and photoluminescence (PL) spectra of the gain media under 532 nm (shown in green dashes) excitation are shown in Figs. 1(a) (1-2). Figures 1(a) (3-5) show the UV-Vis. abs. spectra of the TSN1, TSN2 and TSN3 samples. It can be seen that all the samples exhibit significant absorbance overlapping with both the absorption and PL emission band of R6G. Thus, it opened a good possibility of achieving enhanced amplification of light through resonance energy transfer from surface plasmons; although light reabsorption may also hinder the process in this particular scenario.

Figure 1 (b) shows a typical TEM image of TSN1 sample and from it the triangular shaped silver nanoparticle having a mean edge length of 100 nm can be seen. The TEM images of TSN2 and TSN3 are provided in Fig. S1. Furthermore, Fig. 1(c) shows the COMSOL simulated electric field distribution of the TSN1 under 532 nm excitation. With respect to spherical silver nanoparticle, the sharp edges of TSN1, TSN2 and TSNS3 exhibit larger electric field enhancement (as depicted in Fig. S2), advantageous for RL, which motivated us to employ TSN in the present study.

The schematic of RL experiment setup is shown in Fig. 2. Briefly, a 532 nm Gaussian laser (Spectra Physics, USA) beam having 10 ns pulse duration and 10 Hz repetition rate is passed through a neutral density (ND) filter, followed by a convex lens (f =15 cm), after which the focused beam is directly incident on a quartz cuvette having path length of 10 mm×10 mm, which contains the RL sample. At the focal plane, the beam had a radius of ~50 μm. The RL spectra are captured using a detector, kept at 30^0 angle, w.r.t. the incident beam which is connected with the spectrometer (Research India) through an optical fiber. The cuvette has been kept at slight off-axis direction with respect to the incident beam to prevent capturing any Fabry-Perot type modes by the detector. The energy of the incident laser beam (E_{in}) on the RL sample has been measured by using a pyroelectric photodetector (GENTEC, USA), connected with a pre-amplifier. The concentration of TSN1, TSN2 and TSN3 sample for RL characterization in DMF environment is maintained at ~10^{15} nos./ml of particles. The system has been kept at ambient temperature while doing all the RL experiments.

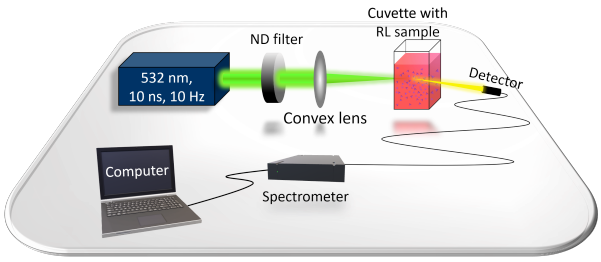

Fig.2. Schematic diagram of the experimental arrangement.

We first employed bare dye solution of R6G in the cuvette, and the used the highest pump energy of~1.74 mJ, as such no narrowing of emission spectra is observed (as shown in Fig. S3). Further typical RL emission spectra obtained in the presence of TSN1, TSN2 and TSN3 samples in the same R6G gain medium are shown in Fig. 3. As shown in Fig. 3 (a), for TSN1 sample, at lower E_{in} values (~0.45 mJ), a broad emission spectrum having a large FWHM is obtained. This broader emission spectrum is a sign of fluorescence, that is, spontaneous emission, from the dye molecules suspended within DMF solution. However, as the E_{in} is increased, the spectrum gets narrowed down at a particular portion of the emission spectrum after a certain E_{in} values. Correspondingly, the integrated area (in a.u.) *vs.* E_{in} graph shows a sudden change in its slope. The intersection point of those 2 slopes is denoted as lasing threshold energy (E_{in}^{th}). In case of TSN1 sample, the

value of E_{in}^{th} is calculated to be 1.27 mJ. Further, the FWHM of the emission spectra also shows a drastic reduction with the increment of E_{in}. The physical mechanisms of RL emission from TSN1 sample basically generates due to random scattering of light [34] within the suspension which increases dwell time of light and increases population inversion and increases the gain and when the overall loss is compensated through the gain, lasing happens. In a similar manner, the gain medium with TSN2 and TSN3 samples are also excited using the same configuration. Figures 3 (b-c) show the corresponding RL emission spectra obtained with TSN2 and TSN3 samples, respectively. It is interesting to note that the values of E_{in}^{th} are found to be 1.06 mJ and 0.78 mJ for TSN2 and TSN3 sample, respectively for the same scatterer concentrations. A 39% reduction of E_{in}^{th} value in TSN3, in compared to those with TSN1 and TSN2, can be attributed to lower values of Emission Overlap (EO) and lower probability of light reabsorption in TSN3 than TSN1 and TSN2. Upon further investigation, it is revealed that, the emission spectrum has an overall shift of 8 nm by changing the system configurations as depicted in **Fig. S2**.

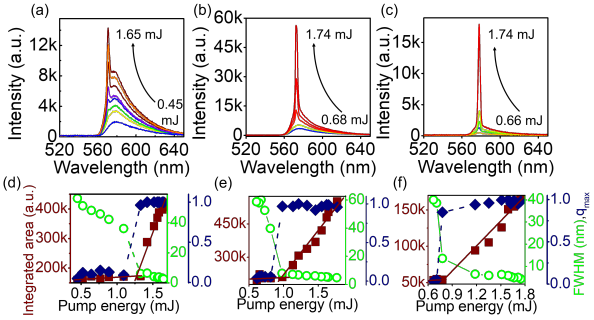

Fig. 3. RL emission spectra for (a) TSN1, (b) TSN2 and (c) TSN3 samples at variable E_{in} values. Variation of integrated area (brown squares), FWHM in nm (green circles) and q_{max} (blue diamonds) at different E_{in} values for (d) TSN1, (e) TSN2 and (f) TSN3 samples.

We now explore for the phenomenon of phase transition of photonic paramagnetic state to RSB spin glass state in our RL system. According to the RSB theory, for quenched disorder, each laser shot will generate a replica, i.e., a copy of the RL system under identical experimental circumstances. By analogy to SGT, each instance of RL emission can be compared to the inherent spin state of the disordered system, and the injected pump energy is comparable with the inverse of temperature [25]. In this situation, one can define an order parameter q (see below), equivalent to the Parisi order parameter in SGT, such that the probability density function (PDF) $P(q)$ can be used to discriminate fluorescence from RL. In case of fluorescence, obtained at low pump energy, the internal modes are not interacting with each other and this is the scenario of photonic paramagnetic phase, where the distribution of PDF is centred at $q = 0$. Now, on increment of input pump energy, inter modal interactions occurs and the intensity of the emitted spectra fluctuates randomly from pulse to pulse. Each spectrum or replica can thus be considered as the intensity configuration of a different state of the same thermodynamic glassy phase. In this high energy glassy phase, all modes interact highly and frustrated by the disorder $|q_{max}|$ assumes all possible values lying in the range [−1, 1].

To investigate RSB in our RL systems, we first conducted an experiment to study the stability of it. Figure 4 (a) shows the RL intensity variation in TSN1 sample for E_{in}=1.74 mJ, where the system is pumped with over 10^4 laser shots at 10 Hz repetition rate. Remarkably, the spectral intensity is found to be nearly stable, with no photodegradation or precipitation observed in the cuvette. Similar results were reported in $ZrTe_2$ based system, where no precipitation was observed and a situation of time-independent system configuration was considered [32]. Further, it may be noted that, during syntheses of TSN1, TSN2 and TSN3 scatterer particles, Polyvinylpyrrolidone (PVP) is used as capping agent for achieving surface stabilization. The literature reports confirmed that PVP and DMF can form hydrogen bond between themselves and also there will be strong dipole−dipole interaction between PVP and DMF [35, 36]. These strong interactions between PVP and DMF creates a network of highly stable disordered media within which TSNs acts as scattering centers and optical gain is provided from the dye molecules. We propose that, due to this networking of stable structure, the effective viscosity of the medium will be very large and thus the Brownian motion and precipitation will be severely hindered during the time of observation of RSB feature, as also observed earlier by Pincheira *et al.* in amorphous TiO_2 [31]. Some detailed calculations in this regard are given in the Supplementary information. Experimentally also we observed no precipitation or degradation of the sample and the RL intensity remains stable as shown in Fig. 4 (a).

Admittedly, the internal phase information of the lasing modes is difficult in acquiring during experiments, which makes evaluation of replicas of the laser modes complicated. However, the intensity magnitudes can be experimentally determined which gives valuable information about the RL modes. Henceforth, for identifying RSB in our system, we conducted a statistical study by acquiring N_s = 1000 single shot emission spectra (replicas) with spectrometer having 100 ms time delay between two succeeding spectra for calculating the spectral intensity variations. If k represents an index for a particular wavelength, the average spectral intensity for a particular k-value is given by:

$$\bar{I}(k) = \frac{\sum_{\alpha=1}^{N_s} I_\alpha(k)}{N_s} \qquad (1),$$

Where, $I_\alpha(k)$ is the spectral intensity for α-th replica at k-th indexed wavelength. Thus, the spectral intensity fluctuation for a given wavelength is defined as,

$$\Delta_\alpha(k) = I_\alpha(k) - \bar{I}(k). \qquad (2),$$

Hence, the Parisi overlap parameter (q) for correlating pulse-to-pulse intensity fluctuation of RL is given by,

$$q_{\alpha\beta} = \frac{\sum_{k=1}^{N} \Delta_\alpha(k)\Delta_\beta(k)}{\left[\sqrt{\sum_{k=1}^{N} \Delta_\alpha^2(k)}\right]\left[\sqrt{\sum_{k=1}^{N} \Delta_\beta^2(k)}\right]}, \qquad (3),$$

where, $\alpha, \beta = 1, 2, 3, \ldots\ldots, N_s$ represent the replica labels.

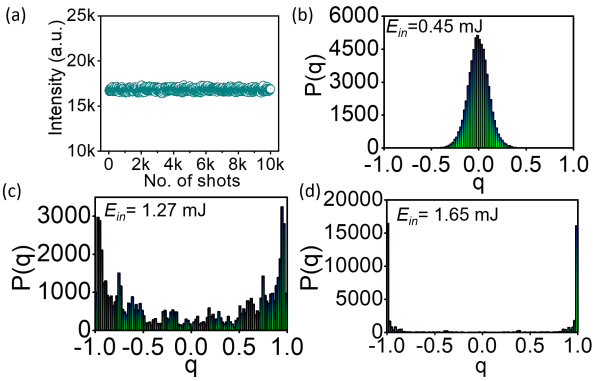

Fig. 4. (a) Variation of RL intensity as a function of the number of shots, under 10 Hz repetition rate for TSN1 sample above threshold energy E_{in} = 1.74 mJ, depicting no photo degradation. Distributions of the overlap parameter q at pump energies of (b) 0.45 mJ, (c) 1.27 mJ and (d) 1.65 mJ, for TSN1 sample.

The PDF $P(q)$ data in Fig. 4 are plotted taking a bin size of 0.02. As shown in Figs. 4(b), for TSN1 sample, at below E_{in}^{th} (E_{in}=0.45 mJ), the PDF consists its maximum value at q_{max}=0. In this scenario, the emission intensities at various wavelengths are highly uncorrelated, which signifies the spontaneous emission behaviour at lower input energies, corresponding to paramagnetic regime in thermodynamics. However, at E_{in}=1.27 mJ, as shown in Fig. 4 (c), the PDF broadens and its maxima switches with correspondingly to a value $|q_{max}|\neq 0$. This implies that the modes are getting coupled with each other within the RL system and it grows stronger with increasing energy, resulting in a bimodal shape of PDF plots, signifying spin-glass phase transition. This shift from the paramagnetic domain to the spin-glass phase is the central characteristic of the RSB transition. Hence, this evolution in q_{max} indicates the transition between fluorescence to RL behaviour in TSN1 sample, which almost coincides with the FWHM narrowing of the spectra obtained in Fig. 3(d). Further, Fig. 3 (d) (blue diamonds) shows the change of q_{max} with change in E_{in} for TSN1 sample. In a similar fashion, Fig. 4(d) represents a fully transformed RSB domain in the colloidal plasmonic RL. The phase transformation PDF plots for TSN2 and TSN3 samples are shown in Fig. S5. Interestingly, there is a prominent change in the $|q_{max}|$ value near the lasing threshold for TSN2 and TSN3 samples as well. So, the present report unveils the new insights into the novel realm of RLs through SGT and predetermines its lasing parameters through the reported method.

In summary, herein we have reported a colloidal plasmonic RL system, comprising of exotic metal nanoparticles of TSN1, TSN2 and TSN3 used as scatterers. The randomly distributed scattering media emits RL emission in the visible region of 570-578 nm, having very low linewidth of 3-6 nm through rich light-matter interaction by providing plasmonic enhancement and scattering. A ~39% reduction in lasing threshold values is reported by interchanging the scatterer components, within the amplifying medium. Moreover, as evident from the probability distribution of order parameter, the phenomenon of RSB is reported for the first time in a colloidal plasmonic RL system. Thus, this report demonstrates the RSB phenomenon in a colloidal plasmonic RL system experimentally.

Funding. Department of Science & Technology and Biotechnology, Government of West Bengal (332(sanc.)/ST/P/S&T/16G-24/2018, dt. March 06, 2019); UGC, Govt. of India CAS-II programme [No. F.530/20/CAS-II/2018(SAP-I)]; FIST Programme of DST, Govt. of India [No. SR/FST/PS-II/2018/52(c)].

Acknowledgments. A. Dey acknowledges Ministry of Education, Government of India, NIT Durgapur for providing the maintenance fellowship. The authors thank Indian Science Technology and Engineering facilities Map (I-STEM), a program supported by Office of the Principal Scientific Advisor to the Govt. of India, for enabling access to the COMSOL Multiphysics 6.0 software suite used to carry out this work.

Disclosures. The authors declare no conflicts of interest.

Data availability. Data underlying the results presented in this Letter are not publicly available at this time but may be obtained from the authors upon reasonable request.

Supplemental document. See Supplement 1 for supporting content.

References

1. R. Sapienza, Nat. Rev. Phys. **1,** 690 (2019).
2. D.S. Wiersma, and A. Lagendijk, Phys. Rev. E **54**, 4256 (1996).
3. B. Kumar, R. Homri, S.K. Maurya, M. Lebental, and P. Sebbah, Optica **8,** 1033 (2021).
4. S. Gottardo, S. Cavalieri, O. Yaroshchuk, and D.S. Wiersma, Phys. Rev. Lett. **93,** 263901 (2004).
5. S. Mujumdar, M. Ricci, R. Torre, and D.S. Wiersma, Phys. Rev. Lett. **93**, 053903 (2004).
6. H. Cao, Y.G. Zhao, X. Liu, E.W. Seelig, and R.P.H. Chang, Appl. Phys. Lett. **75**, 1213 (1999).
7. A. Pramanik, S. Biswas, P. Kumbhakar, and P. Kumbhakar, J. Lumin. **230**, 117720 (2021).
8. V. Letokhov, Sov. Phys. JETP **26**, 835 (1968).
9. T. Zhai, X. Zhang, Z.Pang, X. Su, H. Liu, S. Feng, and L. Wang, Nano Lett. **11,** 4295 (2011).
10. Y. Ni, H. Wan, W. Liang, S. Zhang, X. Xu, L. Li, Y. Shao, S. Ruan, and W. Zhang, Nanoscale **13**, 16872 (2021).
11. S.W. Chen, J.Y. Lu, B.Y. Hung, M. Chiesa, P.H. Tung, J.H. Lin, and T.C.K. Yang, Opt. Express **29**, 2065 (2021).
12. B. Xu, Z. Gao, Y. Wei, Y. Liu, X. Sun, W. Zhang, X. Wang, Z. Wang, and X. Meng, Nanoscale **12,** 4833 (2020).
13. Y. Liu, W. Yang, S. Xiao, N. Zhang, Y. Fan, G. Qu, and Q. Song, ACS Nano **13,** 10653-10661 (2019).
14. W. Gao, T. Wang, J. Xu, P. Zeng, W. Zhang, Y. Yao, C. Chen, M. Li, and S.F. Yu, Small **17**, 2103065 (2021).
15. I.B. Dogru-Yuksel, C. Jeong, B. Park, M. Han, J.S. Lee, T.I. Kim, and S. Nizamoglu, Adv. Funct. Mater. **31**, 2104914 (2021).
16. S. Kim, S. Yang, S.H. Choi, Y.L. Kim, W. Ryu, and C. Joo, Sci. Rep. **7**, 4506 (2017).
17. A. Dey, A. Pramanik, P. Kumbhakar, S. Biswas, S.K. Pal, S.K. Ghosh, and P. Kumbhakar, OSA Contin. **4**, 1712 (2021).
18. D. Zhang, G. Kostovski, C. Karnutsch, and A. Mitchell, Org. Electron. **13,** 2342 (2012).
19. E. Vasileva, Y. Li, I. Sychugov, M. Mensi, L. Berglund, and S. Popov, Adv. Opt. Mater. **5**, 1700057 (2017).
20. S. Biswas, and P. Kumbhakar, Nanoscale, **9**, 18812 (2017).
21. T. Zhai, J. Chen, L. Chen, J. Wang, L. Wang, D. Liu, S. Li, H. Liu, and X. Zhang, Nanoscale **7**, 2235 (2015).
22. J. Zhang, Z. Li, Y. Bai, and Y. Yin, Appl. Mater. Today **26**, 101358 (2022).
23. Y. Wan, H. Wang, H. Li, R. Ye, X. Zhang, J. Lyu, and Y. Cai, Opt. Express, **30**, 8222 (2022).
24. M. Mézard, G. Parisi, and M.A. Virasoro, Spin glass theory and beyond: An Introduction to the Replica Method and Its Applications (World Scientific,1987).
25. N. Ghofraniha, I. Viola, F. Di Maria, G. Barbarella, G. Gigli, L. Leuzzi, and C. Conti, Nat. Commun. **6**, 6058 (2015).
26. A. Sarkar, B.S. Bhaktha, and J. Andreasen, Sci. Rep. **10**, 2628 (2020).
27. E.D. Coronel, M.L. da Silva-Neto, A.L. Moura, I.R. González, R.S. Pugina, E.G. Hilário, E.G. da Rocha, J.M.A. Caiut, A.S. Gomes, and E.P. Raposo, Sci. Rep. **12**,1051 (2022).
28. A.S. Gomes, E.P. Raposo, A.L. Moura, S.I. Fewo, P.I. Pincheira, V. Jerez, L.J. Maia, and C.B. de Araújo, Sci. Rep. **6**, 27987 (2016).
29. Tommasi, E. Ignesti, S. Lepri, and S. Cavalieri, Sci. Rep. **6,** 37113 (2016).
30. S. Basak, A. Blanco, and C. López, Sci. Rep. **6,** 1 (2016).
31. P.I. Pincheira, A.F. Silva, S.I. Fewo, S.J. Carreño, A.L. Moura, E.P. Raposo, A.S. Gomes, and C.B. de Araújo, Opt. Lett. **41**, 3459 (2016).
32. P.I. Pincheira, M.L. da Silva Neto, M. Maldonado, C.B. de Araujo, A.M. Jawaid, R. Busch, A.J. Ritter, R.A. Vaia, and A.S. Gomes, Nanoscale **12,** 15706 (2020).
33. K. Mondal, S. Biswas, T. Singha, S.K. Pal, P.K. Datta, S.K. Ghosh, and P. Kumbhakar, Opt. Lett. **46**, 4879 (2021).
34. A. Dey, A. Pramanik, S. Biswas, U. Chatterjee, and P. Kumbhakar, J. Lumin. **251**, 119252 (2022).
35. A. Kedia, and P.S. Kumar, J. Phys. Chem. C **116**, 23721 (2012).
36. K.M. Koczkur, S. Mourdikoudis, L. Polavarapu, and S.E. Skrabalak, Dalton Trans. **44**, 17883 (2015).

Article Thumbnail:

References

1. R. Sapienza, Determining random lasing action, Nat. Rev. Phys. **1,** 690 (2019).
2. D.S. Wiersma, and A. Lagendijk, Light diffusion with gain and random lasers, Phys. Rev. E **54**, 4256 (1996).
3. B. Kumar, R. Homri, S.K. Maurya, M. Lebental, and P. Sebbah, Localized modes revealed in random lasers, Optica **8,** 1033 (2021).
4. S. Gottardo, S. Cavalieri, O. Yaroshchuk, and D.S. Wiersma, Quasi-two-dimensional diffusive random laser action, Phys. Rev. Lett. **93,** 263901 (2004).
5. S. Mujumdar, M. Ricci, R. Torre, and D.S. Wiersma, Amplified extended modes in random lasers, Phys. Rev. Lett. **93**, 053903 (2004).
6. H. Cao, Y.G. Zhao, X. Liu, E.W. Seelig, and R.P.H. Chang, Effect of external feedback on lasing in random media, Appl. Phys. Lett. **75**, 1213 (1999).
7. A. Pramanik, S. Biswas, P. Kumbhakar, and P. Kumbhakar, External feedback assisted reduction of the lasing threshold of a continuous wave random laser in a dye doped polymer film and demonstration of speckle free imaging, J. Lumin. **230**, 117720 (2021).
8. V. Letokhov, Generation of light by a scattering medium with negative resonance absorption, Sov. Phys. JETP **26**, 835 (1968).
9. T. Zhai, X. Zhang, Z.Pang, X. Su, H. Liu, S. Feng, and L. Wang, Random laser based on waveguided plasmonic gain channels, Nano Lett. **11,** 4295 (2011).
10. Y. Ni, H. Wan, W. Liang, S. Zhang, X. Xu, L. Li, Y. Shao, S. Ruan, and W. Zhang, Random lasing carbon dot fibers for multilevel anti-counterfeiting, Nanoscale **13**, 16872 (2021).
11. S.W. Chen, J.Y. Lu, B.Y. Hung, M. Chiesa, P.H. Tung, J.H. Lin, and T.C.K. Yang, Random lasers from photonic crystal wings of butterfly and moth for speckle-free imaging, Opt. Express **29**, 2065 (2021).
12. B. Xu, Z. Gao, Y. Wei, Y. Liu, X. Sun, W. Zhang, X. Wang, Z. Wang, and X. Meng, Dynamically wavelength-tunable random lasers based on metal–organic framework particles, Nanoscale **12,** 4833 (2020).
13. Y. Liu, W. Yang, S. Xiao, N. Zhang, Y. Fan, G. Qu, and Q. Song, Surface-emitting perovskite random lasers for speckle-free imaging, ACS Nano **13,** 10653-10661 (2019).
14. W. Gao, T. Wang, J. Xu, P. Zeng, W. Zhang, Y. Yao, C. Chen, M. Li, and S.F. Yu, Robust and Flexible Random Lasers Using Perovskite Quantum Dots Coated Nickel Foam for Speckle‐Free Laser Imaging, Small **17**, 2103065 (2021).
15. I.B. Dogru-Yuksel, C. Jeong, B. Park, M. Han, J.S. Lee, T.I. Kim, and S. Nizamoglu, Silk Nanocrack Origami for Controllable Random Lasers, Adv. Funct. Mater. **31**, 2104914 (2021).
16. S. Kim, S. Yang, S.H. Choi, Y.L. Kim, W. Ryu, and C. Joo, Random lasing from structurally-modulated silk fibroin nanofibers, Sci. Rep. **7**, 4506 (2017).
17. A. Dey, A. Pramanik, P. Kumbhakar, S. Biswas, S.K. Pal, S.K. Ghosh, and P. Kumbhakar, Manoeuvring a natural scatterer system in random lasing action and a demonstration of speckle free imaging, OSA Contin. **4**, 1712 (2021).
18. D. Zhang, G. Kostovski, C. Karnutsch, and A. Mitchell, Random lasing from dye doped polymer within biological source scatters: The pomponia imperatorial cicada wing random nanostructures, Org. Electron. **13,** 2342 (2012).
19. E. Vasileva, Y. Li, I. Sychugov, M. Mensi, L. Berglund, and S. Popov, Lasing from organic dye molecules embedded in transparent wood, Adv. Opt. Mater. **5**, 1700057 (2017).
20. S. Biswas, and P. Kumbhakar, Continuous wave random lasing in naturally occurring biocompatible pigments and reduction of lasing threshold using triangular silver nanostructures as scattering media, Nanoscale, **9**, 18812 (2017).
21. T. Zhai, J. Chen, L. Chen, J. Wang, L. Wang, D. Liu, S. Li, H. Liu, and X. Zhang, A plasmonic random laser tunable through stretching silver nanowires embedded in a flexible substrate, Nanoscale **7**, 2235 (2015).
22. J. Zhang, Z. Li, Y. Bai, and Y. Yin, Gold nanocups with multimodal plasmon resonance for quantum-dot random lasing, Appl. Mater. Today **26**, 101358 (2022).
23. Y. Wan, H. Wang, H. Li, R. Ye, X. Zhang, J. Lyu, and Y. Cai, Low-threshold random lasers enhanced by titanium nitride nanoparticles suspended randomly in gain solutions. Opt. Express, **30**, 8222 (2022).
24. M. Mézard, G. Parisi, and M.A. Virasoro, Spin glass theory and beyond: An Introduction to the Replica Method and Its Applications (World Scientific,1987).
25. N. Ghofraniha, I. Viola, F. Di Maria, G. Barbarella, G. Gigli, L. Leuzzi, and C. Conti, Experimental evidence of replica symmetry breaking in random lasers, Nat. Commun. **6**, 6058 (2015).
26. A. Sarkar, B.S. Bhaktha, and J. Andreasen, Replica symmetry breaking in a weakly scattering optofluidic random laser, Sci. Rep. **10**, 2628 (2020).
27. E.D. Coronel, M.L. da Silva-Neto, A.L. Moura, I.R. González, R.S. Pugina, E.G. Hilário, E.G. da Rocha, J.M.A. Caiut, A.S. Gomes, and E.P. Raposo, Simultaneous evaluation of intermittency effects, replica symmetry breaking and modes dynamics correlations in a Nd: YAG random laser, Sci. Rep. **12**,1051 (2022).
28. A.S. Gomes, E.P. Raposo, A.L. Moura, S.I. Fewo, P.I. Pincheira, V. Jerez, L.J. Maia, and C.B. de Araújo, Observation of Lévy distribution and replica symmetry breaking in random lasers from a single set of measurements, Sci. Rep. **6**, 27987 (2016).
29. F. Tommasi, E.Ignesti, S. Lepri, and S. Cavalieri, Robustness of replica symmetry breaking phenomenology in random laser. Sci. Rep. **6,** 37113 (2016).
30. S. Basak, A. Blanco, and C. López, Large fluctuations at the lasing threshold of solid-and liquid-state dye lasers, Sci. Rep. **6**, 1 (2016).
31. P.I. Pincheira, A.F. Silva, S.I. Fewo, S.J. Carreño, A.L. Moura, E.P. Raposo, A.S. Gomes, and C.B. de Araújo, Observation of photonic paramagnetic to spin-glass transition in a specially designed TiO_2 particle-based dye-colloidal random laser, Opt. Lett. **41**, 3459 (2016).
32. P.I. Pincheira, M.L. da Silva Neto, M. Maldonado, C.B. de Araujo, A.M. Jawaid, R. Busch, A.J. Ritter, R.A. Vaia, and A.S. Gomes, Monolayer 2d $ZrTe_2$ transition metal dichalcogenide as nanoscatter for random laser action, Nanoscale **12,** 15706 (2020).
33. K. Mondal, S. Biswas, T. Singha, S.K. Pal, P.K. Datta, S.K. Ghosh, and P. Kumbhakar, Unusual higher-order nonlinear optical properties in Au-coated triangular Ag-Au nanostructures, Opt. Lett. **46**, 4879 (2021).
34. A. Dey, A. Pramanik, S. Biswas, U. Chatterjee, and P. Kumbhakar, Tunable and low-threshold random lasing emission in waveguide aided Rhodamine-6G dye incorporated silica embedded thin films, J. Lumin. **251**, 119252 (2022).
35. A. Kedia, and P.S. Kumar, Solvent-adaptable poly (vinylpyrrolidone) binding induced anisotropic shape control of gold nanostructures. J. Phys. Chem. C **116**, 23721 (2012).
36. K.M. Koczkur, S. Mourdikoudis, L. Polavarapu, and S.E. Skrabalak, Polyvinylpyrrolidone (PVP) in nanoparticle synthesis, Dalton Trans. **44**, 17883 (2015).